Electron Self-Exchange in Redox Polymers. 2. A Study of Ion Aggregation and Intermolecular Interactions

R. Aldrin Denny and M. V. Sangaranarayanan*

Department of Chemistry, Indian Institute of Technology, Madras, 600 036 India

Received: January 28, 1998; In Final Form: May 27, 1998

The diffusion−migration equation (derived in part 1) is subjected to the analysis of steady-state current−potential responses and the effects of intermolecular interaction between neighboring particles and ion association between the electroactive and electroinactive species on maximal limiting current and the corresponding redox composition are studied both in the presence and absence of site diluent. The variation of the apparent diffusion coefficient with molar fraction of redox active species is analyzed as a function of the ion pairing constant and interaction energetics. The steady-state analysis suggests that the transport equation is valid only for a small region of interaction energy and breaks down when its value exceeds the order of k_BT. The possibility of phase separation in redox polymers is also discussed.

1. Introduction

Ion pair formation involving electroactive species and counterions is now a well-known phenomena in a large class of ionomeric systems.[1−9] The influence of ion pair formation and intermolecular interactions between the electroactive species has not yet been simultaneously analyzed in detail in chemically modified electrodes. However, few isolated investigations exist in the context of charge transport in redox polymers for studying conductance, redox capacity, and diffusion coefficient variation with interaction energy and no systematic study starting from the diffusion−migration equation, relating the observable current responses to the interaction energy and ion pairing, is available. One of the earliest methods of calculating current when interaction effects are present is due to Laviron et al.[10] wherein current is explicitly reported in terms of potential and interaction coefficients using an approach analogous to Frumkin isotherm for adsorption of species. We have recently employed[8,11−13] kinetic Ising model and irreversible thermodyanmics versions to derive transport equations, assuming all the redox species present are electron transfer active (i.e., for systems without ion pairing). When ion pairing is present, not all the redox species present in the lattice are electron transfer active but only those which exist as ions (whose concentration is governed by the ion association equilibrium constant) can transport charge. Consequently in part 1, we have employed the kinetic Ising model framework to include ion pairing between the electroactive ions and counterionic species, and we have reported the appropriate spatiotemporal diffusion−migration equation indicating that the structure of the transport equation is nontrivial when ion pairing and interaction energies are influences.

Here we investigate the coupling of electroactive oxidized and reduced species as well as electroactive ion−electroinactive counterion coupling inside the redox polymer on steady state current−potential responses. Section 2 deals with the steady state current responses for the diffusion−migration equation obtained in part 1. The variation of current with ion−redox species association constant and nearest neighboring interaction is also studied. In section 3, we discuss the variation of diffusion coefficient with fractional occupancy of redox species. The competing effects of association constant and interaction energetics is demonstrated. Section IV provides a few perspectives.

2. Steady State Solution of the Diffusion−Migration Equation

We consider a polymeric redox sample poised between two parallel plane electrodes spanning the region between $x = 0$ and $x = l$, where l is the thickness of the polymer film attached. The steady state flux for a single electron transport is given by (cf. eq 36 of part 1)

$$\frac{I}{F} = -J_A = J_B = D_E\left\{\chi_B\frac{\partial\chi_A}{\partial x} - \chi_A\frac{\partial\chi_B}{\partial x} + \frac{e}{k_BT}\chi_A\chi_B\frac{\partial\Phi}{\partial x} + \frac{J}{k_BT}\chi_A\chi_B\frac{\partial\chi_A}{\partial x}\right\} \quad (1)$$

Assuming current due to electroinactive counterion as zero,

$$0 = \frac{\partial\chi_C}{\partial x} - \frac{e}{k_BT}\chi_C\frac{\partial\Phi}{\partial x} \quad (2)$$

The other obvious relations arising from the electroactive species conservation, electroneutrality and ion association equilibria are $\chi_A + \chi_B + \chi_D = 1$, $\chi_A = \chi_C$, and $\chi_D = \kappa\chi_A\chi_C$ respectively, where $\kappa = KC_E^0$ and K ($=k_{as}/k_{dis}$) denotes the ion association equilibrium constant. The potential difference between the two electrodes can be represented as[14]

$$E = \frac{k_BT}{e}\ln\frac{\chi_{A_{x=l}}\chi_{B_{x=0}}}{\chi_{A_{x=0}}\chi_{B_{x=l}}} + \Phi_l - \Phi_0 \quad (3)$$

where the last two terms denote the potentials at the two ends of the film (i.e., at $x = l$ and x = 0), respectively.

In addition, the film is conserved in χ_B and $\chi_A + \chi_D$. Thus, for example,

$$\int_0^l \chi_B dx = \frac{\rho}{1+\rho} \quad (4)$$

10.1021/jp980924x CCC: $15.00
Published on Web 10/13/1998

or equivalently

$$\int_0^l (\chi_A + \kappa\chi_A^2)dx = \frac{1}{1+\rho} \quad (5)$$

where ρ is the starting ratio of reduced over oxidized redox site concentration that defines the redox composition of the film.

The problem is simplified if we employ dimensionless variables and parameters: $y = x/l$, $\psi = I/I_d$, $I_d = eC_E^0D_E/l$, $\phi = (e/k_BT)\Phi$, $\lambda = (e/k_BT)E$, and $\epsilon = J/k_BT$. Thus eqs 1 and 2 become,

$$\psi = \chi_B\frac{\partial\chi_A}{\partial y} - \chi_A\frac{\partial\chi_B}{\partial y} + \chi_A\chi_B\frac{\partial\phi}{\partial y} + \epsilon\chi_A\chi_B\frac{\partial\chi_A}{\partial y} \quad (6)$$

and

$$0 = \frac{\partial\chi_C}{\partial y} - \chi_C\frac{\partial\phi}{\partial y} \quad (7)$$

respectively. We rewrite eq 3 as

$$\lambda = \ln\frac{\chi_{A_1}\chi_{B_0}}{\chi_{A_0}\chi_{B_1}} + \phi_1 - \phi_0 \quad (8)$$

where the subscript 0 and 1 refers to $y = 0$ and $y = 1$, respectively.

In order to obtain current, the potential drop $\phi_1-\phi_0$ in eq 8 is expressed using eq 7 as

$$\phi_1 - \phi_0 = \int_0^1 d\phi = \int_0^1 \frac{\partial\chi_C}{\chi_C}$$

From the electroneutrality relation, it follows that

$$\phi_1 - \phi_0 = \int_0^1 \frac{d\chi_A}{\chi_A} = \ln\frac{\chi_{A_1}}{\chi_{A_0}} \quad (9)$$

Thus eq 8 can be rewritten as

$$\lambda = \ln\frac{\chi_{A_1}^2\chi_{B_0}}{\chi_{A_0}^2\chi_{B_1}} \quad (10)$$

Taking into account the conservation of redox species, electroneutrality principle, ion association equilibria, and diffusive and (electric) field assisted movement of counterions, we obtain

$$\psi = [\,2 + (\epsilon - 1)\chi_A - \epsilon\chi_A^2 - \epsilon\kappa\chi_A^3]\frac{d\chi_A}{dy} \quad (11)$$

Integration of the above equation between 0 to y leads to

$$\psi y = 2(\chi_A - \chi_{A_0}) + (\epsilon - 1)\frac{\chi_A^2 - \chi_{A_0}^2}{2} - \epsilon\frac{\chi_A^3 - \chi_{A_0}^3}{3} - \epsilon\kappa\frac{\chi_A^4 - \chi_{A_0}^4}{4} \quad (12)$$

while that between 0 to 1 yields

$$\psi = 2(\chi_{A_1} - \chi_{A_0}) + (\epsilon - 1)\frac{\chi_{A_1}^2 - \chi_{A_0}^2}{2} - \epsilon\frac{\chi_{A_1}^3 - \chi_{A_0}^3}{3} - \epsilon\kappa\frac{\chi_{A_1}^4 - \chi_{A_0}^4}{4} \quad (13)$$

where χ_{A_0} and χ_{A_1} are the surface ($y = 0$) and end ($y = 1$) fractional concentrations of electroactive species A. The above equation gives the current-potential relation in terms of redox concentrations χ_{A_0} and χ_{A_1}, and the next step is to derive current in terms of the initial redox composition of the film. From eq 11 we can write

$$\psi\chi_A dy = [2\chi_A + (\epsilon - 1)\chi_A^2 - \epsilon\chi_A^3 - \epsilon\kappa\chi_A^4]d\chi_A \quad (14)$$

and

$$\psi\chi_A^2 dy = [2\chi_A^2 + (\epsilon - 1)\chi_A^3 - \epsilon\chi_A^4 - \epsilon\kappa\chi_A^5]d\chi_A \quad (15)$$

Thus integrating eqs 14 and 15 between y = 0 and 1 we obtain

$$\int_0^1 \chi_A dy = \frac{1}{\psi}\left[(\chi_{A_1}^2 - \chi_{A_0}^2) + \frac{(\epsilon-1)}{3}(\chi_{A_1}^3 - \chi_{A_0}^3) - \frac{\epsilon}{4}(\chi_{A_1}^4 - \chi_{A_0}^4) - \frac{\epsilon\kappa}{5}(\chi_{A_1}^5 - \chi_{A_0}^5)\right]$$

$$\int_0^1 \chi_A^2 dy = \frac{1}{\psi}\left[\frac{2}{3}(\chi_{A_1}^3 - \chi_{A_0}^3) + \frac{(\epsilon-1)}{4}(\chi_{A_1}^4 - \chi_{A_0}^4) - \frac{\epsilon}{5}(\chi_{A_1}^5 - \chi_{A_5}^5) - \frac{\epsilon\kappa}{6}(\chi_{A_1}^6 - \chi_{A_0}^6)\right]$$

Further using eq (5),

$$\frac{\psi}{1+\rho} = (\chi_{A_1}^2 - \chi_{A_0}^2) + \left(\frac{\epsilon + 2k - 1}{3}\right)(\chi_{A_1}^3 - \chi_{A_0}^3) + \left(\frac{(\epsilon-1)\kappa - \epsilon}{4}\right)(\chi_{A_1}^4 - \chi_{A_0}^4) - \frac{2\epsilon\kappa}{5}(\chi_{A_1}^5 - \chi_{A_0}^5) - \frac{\epsilon\kappa}{6}(\chi_{A_1}^6 - \chi_{A_0}^6) \quad (16)$$

Elimination of ψ from the above equation using eq 13, leads to

$$\frac{2}{1+\rho} = \left[\frac{1-\epsilon}{2(1+\rho)} + 1\right]\frac{\chi_{A_1}^2 - \chi_{A_0}^2}{(\chi_{A_1} - \chi_{A_0})} + \left[\epsilon + 2\kappa + \frac{\epsilon}{1+\rho} - 1\right]\frac{\chi_{A_1}^3 - \chi_{A_0}^3}{3(\chi_{A_1} - \chi_{A_0})} + \left[(\epsilon-1)\kappa + \frac{\epsilon\kappa}{1+\rho} - \epsilon\right]\frac{\chi_{A_1}^4 - \chi_{A_0}^4}{4(\chi_{A_1} - \chi_{A_0})} - 2\epsilon\kappa\frac{(\chi_{A_1}^5 - \chi_{A_0}^5)}{5(\chi_{A_1} - \chi_{A_0})} - \epsilon\kappa\frac{(\chi_{A_1}^6 - \chi_{A_0}^6)}{6(\chi_{A_1} - \chi_{A_0})} \quad (17)$$

For a given set of values for potential, initial composition, interaction energy and ion pairing constant, we have two unknowns χ_{A_0} and χ_{A_1} from two equations viz eqs 10 and 17 in order to calculate current ψ. Knowing the dimensionless current, the concentration profiles of χ_A can be obtained using eq 12 and that of χ_B, χ_C, and χ_D from the conservation of electroactive species and electroneutrality relations. Subsequently, the potential profile can be obtained using eq 9.

Now we shall investigate some of the features that arise from ion pairing (effects as quantified by κ). The parameters that can be studied under experimental conditions include maximal limiting current (ψ_{LM}) and redox composition of the film (ρ_M) corresponding to ψ_{LM}. The maximal limiting current is obtained when the difference in concentration gradient is maximum (i.e., the concentration of redox active species is completely separated from one end of the polymeric chain (attached to the electrode)

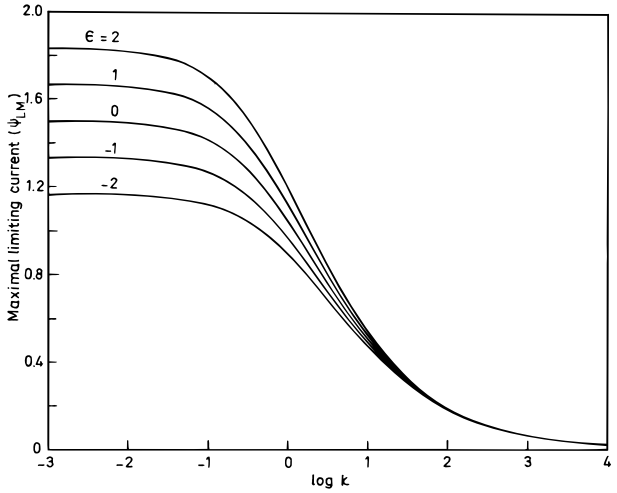

Figure 1. Maximum limiting current ψ_{LM} calculated from eqs 18 and 19 as a function of log κ for various values of interaction energy.

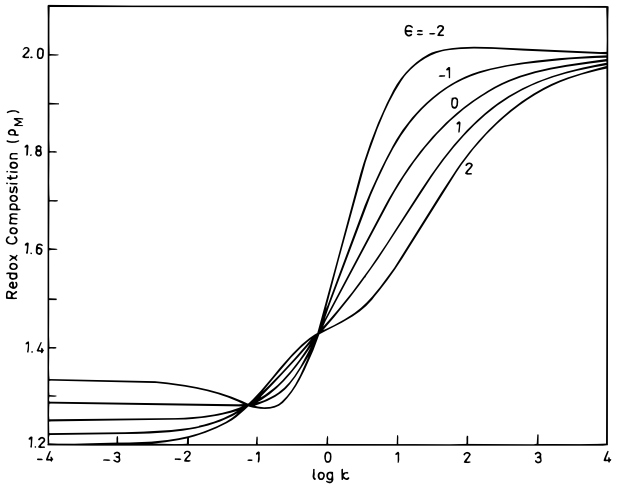

Figure 2. Redox composition corresponding to the maximal limiting current as a function of extent of ion pairing (κ) for the indicated values of interaction energy.

to the other). Under this condition, there will be no A at $y = 0$ and no B at $y = 1$ (i.e., $\chi_{A_0} = 0$ and $\chi_{B_1} = 0$) and hence

$$\chi_{A_1} + \kappa\chi_{A_1}^2 = 1$$

Thus, χ_{A_1} can be written as

$$\chi_{A_1} = \frac{(1 + 4\kappa)^{1/2} - 1}{2\kappa} \tag{18}$$

From eq 13, ψ_{LM} follows as

$$\psi_{LM} = 2\chi_{A_1} + \frac{(\epsilon - 1)}{2}\chi_{A_1}^2 - \frac{\epsilon}{3}\chi_{A_1}^3 - \frac{\epsilon\kappa}{4}\chi_{A_1}^4 \tag{19}$$

and the redox composition ρ_M at the maximal limiting current, ψ_{LM} can be obtained from eq 16 by substituting the above condition:

$$\rho_M = \frac{\psi_{LM}}{\chi_{A_1}^2 + \left[\frac{2\kappa + (\epsilon - 1)}{3}\right]\chi_{A_1}^3 + \left[\frac{(\epsilon - 1)\kappa - \epsilon}{4}\right]\chi_{A_1}^4 - \frac{2\epsilon\kappa}{5}\chi_{A_1}^5 - \frac{\epsilon\kappa}{6}\chi_{A_1}^6} - 1 \tag{20}$$

Figure 1 represents the variation of maximal limiting current with the extent of ion pairing as represented by κ. When the electroinactive counterion C is involved in strong ion pairing with the electroactive species A, ($\kappa \rightarrow \infty$), $\psi_{LM} \rightarrow 2/\kappa^{1/2}$. This is the region where concentration of electroactive species A is less and that of the immobile redox center D is high; however, as mentioned earlier, they do not participate in electron hopping process and hence the maximal current decreases toward zero. When ion pairing between A and C is weak, there will be more number of electron transfer active species A (than D) and thus ψ_{LM} increases and reaches a maximum value at a κ value of about 0.1. For $\kappa \ll 0.1$, almost all the electron hopping inactive species D exists as A and any further decrease in κ does not appreciably change the concentration of A and hence ψ_{LM} remains constant. For low κ value, χ_{A_1} becomes unity and hence

$$\psi_{LM} = \frac{9 + \epsilon}{6}$$

and when interaction between redox active species are assumed to be absent (i.e., $\epsilon = 0$) then $\psi_{LM} \rightarrow 1.5$ as shown by Savéant in an earlier study.[5]

The variation of redox composition corresponding to the maximal limiting current ρ_M, as a function of ion pairing constant κ and interaction energy ϵ, is shown in Figure 2. When ion pairing between A and the electroinactive supporting ion C is strong (large κ), then $\rho_M \rightarrow 2$ and if κ is low, ρ_M decreases to 1.25 when interactions are absent. However, when interaction between redox species exists, ρ_M becomes a function of ϵ, as shown in Figure 2, and at low κ values, is given by

$$\rho_M = \frac{10 + \epsilon}{8 + \epsilon}$$

3. Influence of Electroinactive Supporting Ion

The above analysis pertains to an exact counterbalance of charges between electroactive species A and inactive counterion C (i.e., when the polymer matrix is completely saturated with redox active species). Here we analyze a situation where in addition to redox active species, a monopositive immobile ion F also shares the matrix (called as site diluent). The newly added species (i.e., F is assumed to be electroinactive in the potential range of A/B couple). Thus, when F is adjacent to a redox active site, spin exchange with neighboring site does not occur and the transition probability and the final diffusion−migration equation remains unaltered. However, the diffusion coefficient represented in eq 39 of part 1 needs a modification in the blocking factor, namely, it is necessary to incorporate blocking effects due to the additional species F as well. Thus, electroneutrality and matter conservation laws represented in the earlier section are rewritten for the present situation as, $\chi_A + \chi_F = \chi_C$, $\chi_A + \chi_B + \chi_D = 1$, and $\chi_D = \kappa\chi_A\chi_C$, where χ_F is the concentration ratio of attached electroinactive monopositive ion over the attached electroactive species ($=C_F/C_E^0$). Here we assume that ion pairing exists between electroactive A and electroinactive C and that the attached electroinactive ions F are not involved in ion pairing with counterions.

Current is written using eqs 6 and 7 as

$$\psi = \left[2 + \chi_F + (\epsilon - 1)\chi_A - \frac{\chi_F(\chi_F + 1)}{\chi_A + \chi_F} - \epsilon(1 + \chi_F)\chi_A^2 - \epsilon\kappa\chi_A^3\right]\frac{d\chi_A}{dy} \tag{21}$$

Integrating between the limits 0 and 1, we obtain

$$\psi = (2 + \chi_F)(\chi_{A_1} - \chi_{A_0}) + (\epsilon - 1)\left(\frac{\chi_{A_1}^2 - \chi_{A_0}^2}{2}\right) - \chi_F(\chi_F + 1)\ln\left(\frac{\chi_{A_1} + \chi_F}{\chi_{A_0} + \chi_F}\right) - \epsilon(1 + \kappa\chi_F)\left(\frac{\chi_{A_1}^3 - \chi_{A_0}^3}{3}\right) - \epsilon\kappa\left(\frac{\chi_{A_1}^4 - \chi_{A_0}^4}{4}\right) \quad (22)$$

The conservation of the total amount of oxidized species inside the film for the present set of conditions leads to an equation similar to eq 5 as

$$\int_0^1 [(1 + \kappa\chi_F)\chi_A + \kappa\chi_A^2]dy = \frac{1}{1 + \rho} \quad (23)$$

Using the same procedure as employed earlier we obtain an equation identical to eq 17 incorporating ρ, κ, ϵ, and χ_F with unknown parameters χ_{A_0} and χ_{A_1}. Solving the system of equations simultaneously for a given potential λ and other known parameters (namely ρ, κ, ϵ, and χ_F) leads to the surface and end fractional concentrations of species A and, hence, current, using eq 22. Thus for a series of potential, one can derive current−potential characteristics in addition to various concentration versus potential profiles. Moreover, cathodic limiting current ψ_L, as well as the redox composition of film corresponding to the maximal value of the limiting current ρ_M can also be estimated effortlessly.

The maximal limiting current is obtained when $\chi_{A_0} = 0$ and $\chi_{B_1} = 0$. Now,

$$\chi_{A_1} = \frac{[(1 + \kappa\chi_F)^2 + 4\kappa]^{1/2} - (1 + \kappa\chi_F)}{2\kappa} \quad (24)$$

and

$$\psi_{LM} = (2 + \chi_F)\chi_{A_1} + (\epsilon - 1)\frac{\chi_{A_1}^2}{2} - \chi_F(\chi_F + 1)\ln\left(\frac{\chi_{A_1} + \chi_F}{\chi_F}\right) - \epsilon(1 + \kappa\chi_F)\frac{\chi_{A_1}^3}{3} - \epsilon\kappa\frac{\chi_{A_1}^4}{4} \quad (25)$$

Equations 24 and 25 represent, respectively, fractional concentration of the electroactive species at the end of the film and the maximum limiting current as a function of the system variables.

Figure 3 illustrates the effects of electroinactive diluent F and nature of ion pairing between electroactive ion A and electroinactive counterion C, on the maximal limiting current for different values of interaction energy. As the concentration of F increases, maximal limiting current decreases and also shifts the curve to lower values of ion pairing constant (as measured by κ). The decrease in the tendency of free electroactive ions A to enable ion pairing with electroinactive mobile counterions C arising from the competition between A and F for species C explains this shift. When κ increases, the concentration of A involved in electron transfer decreases, which implies a corresponding increase in the concentration of D which is electron transfer inactive and thus current decreases to zero. When ion pairing nature is not pronounced, ψ_{LM} reaches a limiting value, as expected (cf. Figure 1). Furthermore, from ion pairing equilibria, χ_C has to be a constant suggesting an uniform concentration of electroinactive mobile species C inside the redox polymer and, hence, from eq 7, no spatial variation of charges. Under this condition, diffusion alone contributes to the observed current. The current in this migration-free region obeys $\psi = \chi_{A_0}(t)/\chi_E$ and $\chi_{A_0}(t)$ can be derived from the reversible case using Nernst expression as[15]

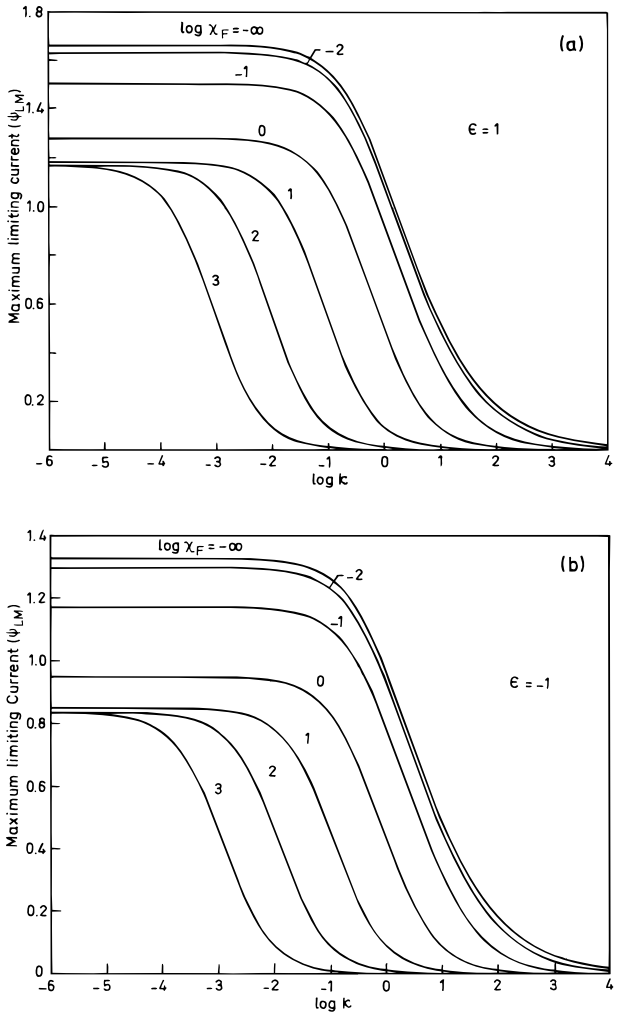

Figure 3. Maximum limiting current ψ_{LM} in the presence of fixed electroinactive ion F and as a function of extent of ion pairing. The numbers on the curves indicate log χ_F values. ϵ in (a) and (b) are +1 and −1, respectively.

$$\chi_{A_0}(t) = \frac{\chi_E}{1 + e^{-\lambda}} \quad (26)$$

Thus, the maximum limiting current becomes a function of interaction energy as

$$\psi_{LM} = \frac{6(1 + \kappa\chi_F)^2 + 3\epsilon(1 + \kappa\chi_F) - 2\epsilon}{6(1 + \kappa\chi_F)^3} \quad (27)$$

When interaction energy is absent,

$$\psi_{LM} = \frac{1}{1 + \kappa\chi_F} \quad (28)$$

as suggested by Savéant.[5] The above analysis demonstrates that the quantitative manner in which interaction energies influence the limiting current cannot be easily foreseen.

The effect of ϵ on ψ_{LM} is shown in Figure 4. A comparison with Figure 1 suggests that ion pairing in the presence of

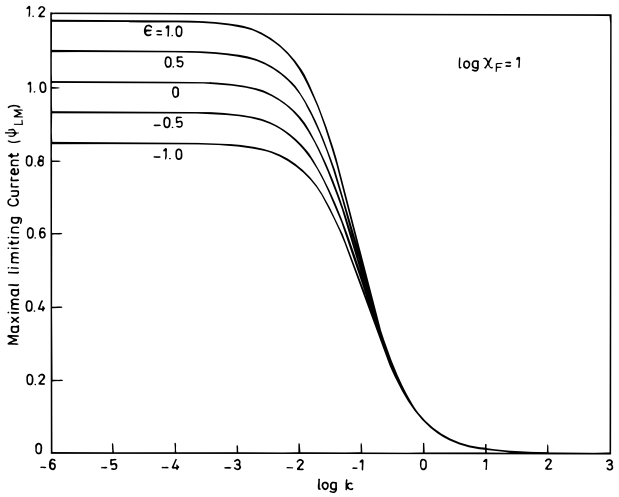

Figure 4. Variation of the maximal limiting current with the extent of ion pairing of electroactive ions (as measured by κ) in the presence of an excess of electroinactive fixed ion (log χ_F) and the extent of interaction (as measured by ϵ). The numbers on the curves are values of ϵ.

electroinactive supporting ion F is more effective than in its absence. The effect of interaction energy upon maximum limiting current remains the same; however, the value of ψ_{LM} is affected due to electroinactive supporting ions.

4. Dependence of Diffusion Coefficient on Molar Fraction of Electroactive Species

Even though Figures 1−4 illustrate the effects of interaction energy, ion pairing, and supporting ion concentration on the maximum limiting current and its corresponding redox composition of the film, the study of parametric dependence of electron hopping diffusion coefficient on concentration of redox active centers is especially illuminating. The molar fraction of redox active sites χ_E is the ratio of electroactive sites to the sum of electroactive and electroinactive sites:[16]

$$\chi_E = \frac{C_E^0}{C_E^0 + C_F} \tag{29}$$

where C_F is the concentration of electroinactive (F) species. The fraction of electroinactive species χ_F in terms of molar fraction of electroactive species is

$$\chi_F = \frac{1 - \chi_E}{\chi_E} \tag{30}$$

The relationship between maximum limiting current i_{LM} and electron hopping diffusion coefficient (D_E^0) and apparent diffusion coefficient (D_E^{ap}) is given by

$$i_{LM} = \frac{eAC_E^0 D_E^{ap}}{l} = \psi_{LM}\frac{eAC_E^0 D_E^0}{l} \tag{31}$$

As shown earlier, under the condition of maximum limiting current, $\chi_{A_0} = 0$ and χ_{A_1} can be written in terms of χ_E and σ as

$$\chi_{A_1} = \frac{\{[1 + \sigma(1 - \chi_E)]^2 + 4\sigma\chi_E\}^{1/2} - [1 + \sigma(1 - \chi_E)]}{2\sigma\chi_E} \tag{32}$$

$\sigma = KC^0$ and $C^0 = C_E^0 + C_F$. From eqs 25 and 31, the ratio

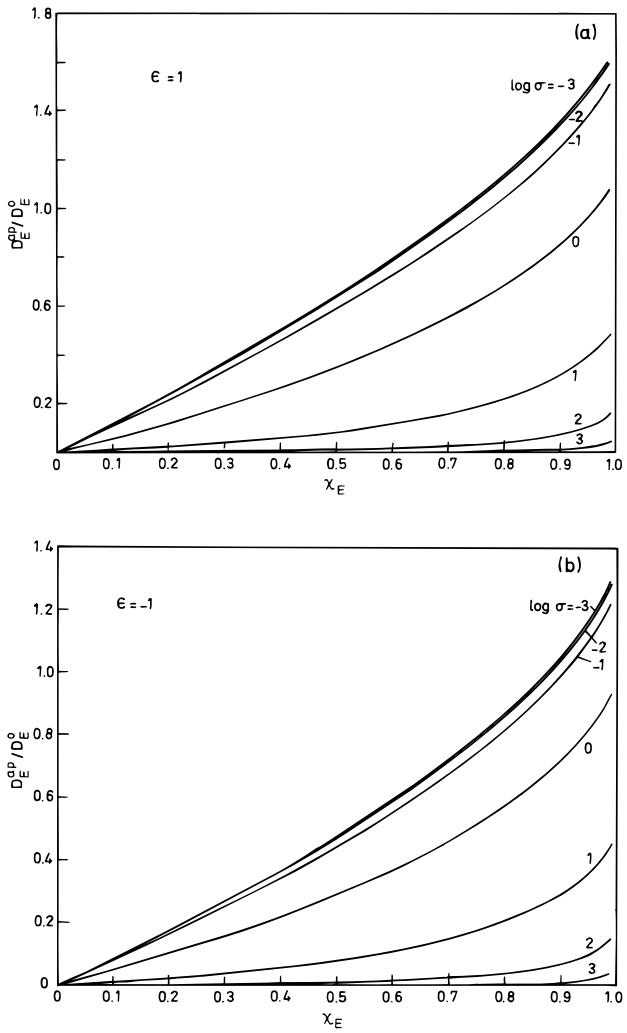

Figure 5. The dependence of the apparent electron hopping diffusion coefficient on the molar fraction of the electroactive species χ_E and the extent of ion pairing as measured by σ. $\epsilon = +1$ (a) and -1 (b), and the numbers on the curves are the values of log σ.

of the electron hopping diffusion coefficients is

$$\frac{D_E^{ap}}{D_E^0} = \left(\frac{1 + \chi_E}{\chi_E}\right)\chi_{A_1} + \frac{(\epsilon - 1)}{2}\chi_{A_1}^2 - \left(\frac{1 - \chi_E}{\chi_E^2}\right)\ln\left(\frac{\chi_E\chi_{A_1} + 1 - \chi_E}{1 - \chi_E}\right) - \epsilon[1 + \sigma(1 - \chi_E)]\chi_{A_1}^3 + \frac{\sigma\epsilon\chi_E\chi_{A_1}^4}{4} \tag{33}$$

Using eqs 32 and 33, the ratio between apparent and actual electron hopping diffusion coefficient, is obtained for various values of ion pairing constant (as measured by σ), interaction energy (ϵ) and molar fraction of electroactive species (χ_E). A plot of D_E^{ap}/D_E^0 with χ_E for various values of σ and ϵ are given in Figures 5 and 6. The variation of apparent electron hopping diffusion coefficient with the fractional concentration of electroactive species is nonlinear, consistent with experimental observations.[16−22] Figure 5 shows that when ion pairing between electroactive A and electroinactive C is weak, indicated by the low value of σ, diffusion coefficient is high and when coupling between A and C becomes stronger the diffusion coefficient ratio falls down quite rapidly suggesting this ratio

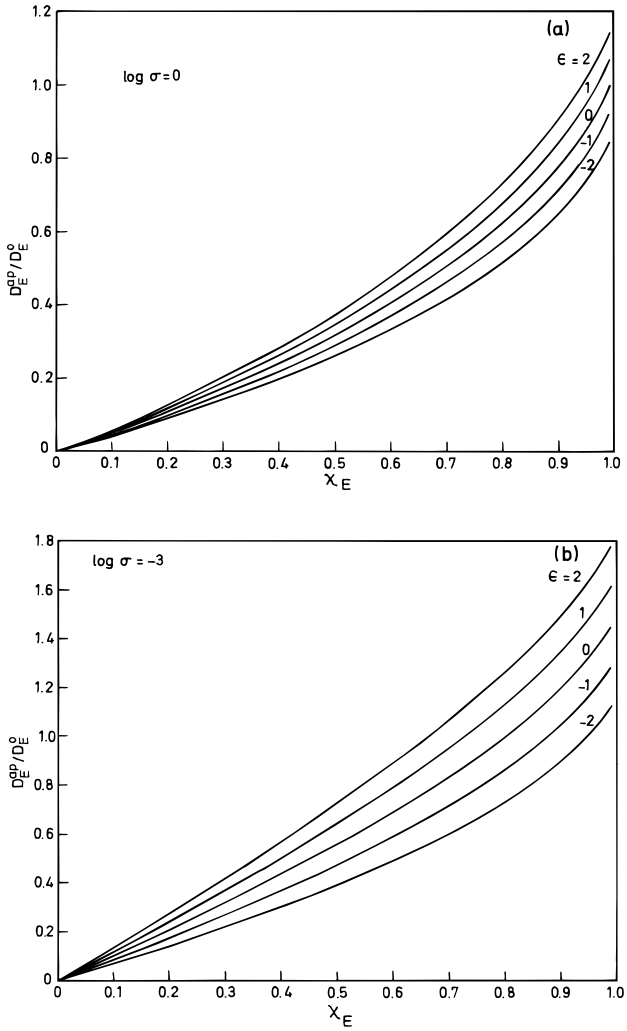

Figure 6. Apparent electron hopping diffusion coefficient variation with the molar fraction of electroactive species χ_E for the indicated values of interaction energy and for ion pairing constant (log σ) values of 0 (a) and -3 (b).

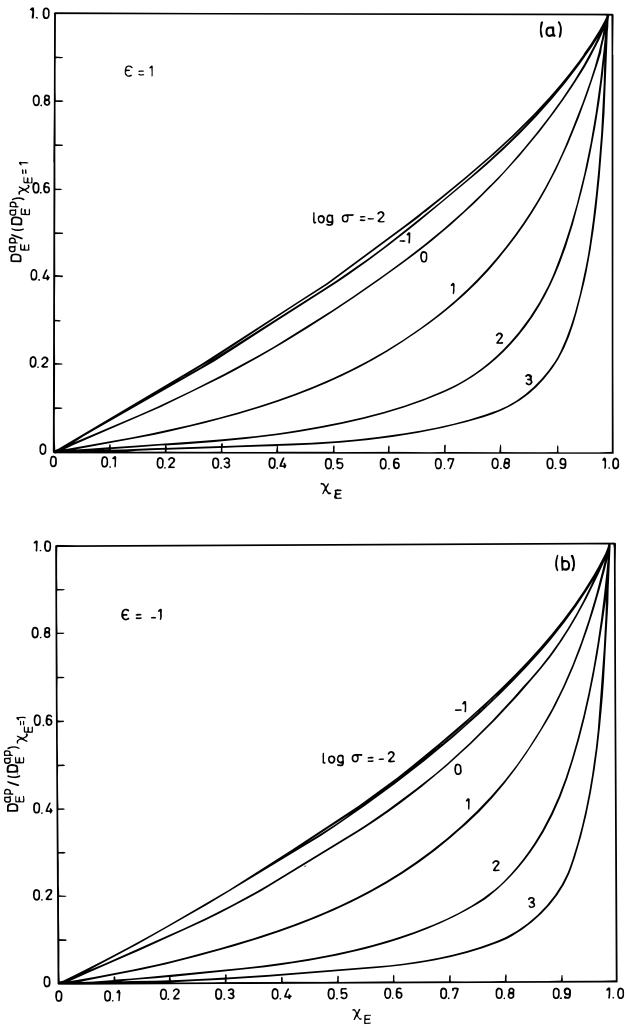

Figure 7. Variation of $D_E^{ap}/(D_E^{ap})_{\chi_{E=1}}$ with the molar fraction of the electroactive species, χ_E, for various values of ion pairing constant (as measured by σ). The values of interaction energy ϵ used in (a) and (b) are $+1$ and -1, respectively. The numbers on the curves indicate the values of log σ.

to be a strong function of ion pairing constant. An earlier study[5] has predicted such variations for noninteracting particles and it is shown here that it is valid even when interaction between particles is considered. For log $\sigma < -2$, the apparent diffusion coefficient becomes independent of ion pairing (i.e., in this region, almost all the redox transfer inactive D present in the system exists as A, which is electroactive and any further decrease in σ does not appreciably change the concentration of A and hence apparent electron hopping diffusion coefficient remains constant). The variation of electron hopping diffusion coefficient with χ_E for various values of ϵ is shown in Figure 6. It suggests that an increase in the interaction energy enhances the value of D_E^{ap}/D_E^0; (however, this influence is significantly dependent on σ. As σ becomes large, the influence of ϵ on electron hopping diffusion coefficient diminishes.

The form of the flux eq 1 is valid only when nearest neighboring interactions J is small comparable with the magnitude of k_BT. When J exceeds the order of k_BT, a quantitatively appropriate treatment is more difficult due to substantial ordering of electron transfer active sites invalidating the earlier assumption in section 3. For instance, when ϵ ($= J/k_BT$) $\gg 0$ (repulsive) then electroactive "like" species (A and A or B and B) avoid one another or electroactive oxidized species A and reduced species B attract each other resulting in *compound formation*, whereas for $\epsilon \ll 0$ (attractive) both oxidized and reduced species group separately leading ultimately to *phase separation*. In the present study, we observed that, for large negative values of ϵ, apparent diffusion coefficient becomes negative suggesting that eq 33 is no longer valid implying the inadequacy of transport eq 1 under this condition. Because the breakdown of eqs 1 and 33 arises from the sign and magnitude of the short range attractive interaction energies, the occurrence of this behavior is attributed to phase separation. When ion pairing between A and counterion C increases, the concentration of free electroactive A decreases, affecting the interactions between electron transfer active oxidized and reduced species resulting finally in shifting the phase separation limit further. Thus, phase separation is a function of both association constant and interaction energy values. Although several earlier reports[23−27] have suggested that phase separation increases the width of current−potential plots, interaction effects are studied here for the first time concerning their role in affecting the diffusion coefficient of the species, maximum limiting current, etc.

Figure 7 represents the normalized plot of apparent electron hopping diffusion coefficient (with respect to $\chi_E = 1$) vs molar fraction of electroactive species for different values of interaction energy and ion pairing constant. Figure 7 suggests a non linear variation of apparent diffusion coefficient with χ_E for higher values of ion pairing constant (σ) and the curve becomes

approximately linear when the ion association is weak. Comparing Figures 7a and 7b it follows that when the interaction between "like" particles (eg., A and A) is repulsive (i.e., when $\epsilon > 0$, $D_E^{ap}/D_E^{ap})_{\chi_E=1}$ variation with χ_E becomes independent of the interaction energy and approaches a linear behavior for lower values of ion pairing association constant). However, when ϵ is decreased, a nonlinear variation is observed. In addition, this comparison also reiterates the earlier observation that the influence of interaction energy is less when ion pairing between the electroactive A and electroinactive C is strong.

5. Perspectives

The investigation of steady state current−potential response suggests ion association of electroactive species with inactive counterions as well as interaction between electron transfer active species to contribute significantly to the rate of charge transport. Maximum limiting current and its corresponding redox composition are shown to be functions of ion pairing constant and interaction energy. The magnitude of the maximum current results from a shift in ion association equilibrium so as to produce a large amount of partially dissociated, oxidized half of redox couple (which is more suited for accepting an electron from the fully associated, reduced half of redox couple) and attractive interaction between electroactive oxidized and reduced species.

The electron transfer inactive ions C and F affect significantly the steady state responses through the ion pairing constant, as measured by KC_E^0, even though their diffusion coefficients are not directly involved in steady state equations. However, effects of these ions are reduced when repulsive interaction between redox species exists. The variation of apparent diffusion coefficient as a function of molar fraction of electroactive species concentration, ion pairing constant (as measured by KC^0) and interaction energy are also studied. A steep increase in the apparent diffusion coefficient arises depending upon the association constant and interaction between electroactive oxidized and its conjugate electron transfer species.

It is imperative here to recall the investigations on phase separation phenomena in diverse contexts[28] so as to point out possible future directions in the field of electrocatalysis. It is customary[29] to study the onset of phase separation in chemical reactions such as

$$A \underset{k_2}{\overset{k_1}{\rightleftharpoons}} B \tag{34}$$

using an order parameter defined in terms of the local concentrations of species A and B, mediated by diverse interaction energetics. The spatial pattern evolves depending upon the range and strength of interactions chosen, and Monte Carlo simulation studies usually employ the Cahn−Hilliard equation with suitable forward and backward reaction rates (k_1 and k_2 above). In the present analysis, the phenomenological equations that describe mechanism I are as follows:

$$A_i + B_j \rightleftharpoons B_i + A_j \tag{35}$$

$$A_j + B_k \rightleftharpoons B_j + A_k \tag{36}$$

along with the appropriate kinetic equations for ion pair formation. The electron hopping mechanism depicted in the eqs 35 and 36 indicate that the rate constants are potential dependent, which in turn are dictated by the site indices.

It is interesting to point out here, that a spin-1 model of the type discussed in section 1 has recently been employed to describe phase separation of amphiphiles in ternary mixtures using Kawasaki spin exchange dynamics via Monte Carlo simulation, in two and three dimensions.[30] Furthermore, Monte Carlo simulation has also been employed to study time dependence of domain size in phase separating binary mixtures.[31] The inclusion of interaction energies in the Hamiltonian (eq 13 of part 1) clearly points to the fact that the occurrence of phase separation is a natural consequence within the theoretical framework developed by us here. An identical conclusion was also reached by Murray[23] for electron hopping in chemically modified electrodes using appropriate chemical potentials. Nevertheless, a quantitative study of phase segregations in such supramolecular structures should commence with clarifying the role of fluctuations and drawing the temperature vs order parameter phase diagram, thereby identifying the coexistence region.[28,29] We do not resort to this sophisticated strategy here especially because of the linearization carried out for exponential terms in potential difference and interaction energies (cf. eqs 26−30 of part 1), while deriving the spatio-temporal transport equation. However, it seems essential to bring into the realm of electrochemistry, these novel phenomena concerning various aspects of phase separation which constitutes currently a frontier arena of statistical physics.

All calculations were performed in a 166 MHz Pentium PC using programs written in MATLAB 4.2 software in the double-precision mode. The number of computation points in each graph varies between 1000 and 5000.

Acknowledgment. Financial support by the Department of Science and Technology, Government of India, is gratefully acknowledged.

Glossary

A	free electroactive oxidized species (monopositive charge)
B	immobile electroactive reduced (neutral) species
C	mobile electroinactive counterion (mononegative charge)
C_E^0	total concentration of electroactive species (mol cm^{-3})
C_F	concentration of electroinactive supporting ion (mol cm^{-3})
D	electron transfer silent oxidized (neutral) species
D_E	electron hopping diffusion coefficient (cm^2 s^{-1})
e	electric charge (C)
E	potential difference (V)
F	immobile electroinactive diluent species (monopositive charge)
I	current density (A cm^{-2})
I_d	diffusion-limited current density (A cm^{-2})
J	interaction energy (J mol^{-1})
k_{as}	association rate constant (cm^3 mol^{-1} s^{-1})
k_{dis}	dissociation rate constant (s^{-1})
k_B	Boltzmann constant (J K^{-1})
k_{ij}	spin-exchange frequency between sites i and j (s^{-1})
k_0	potential dependent spin exchange frequency (s^{-1})
k_0^C	counterion hopping frequency (s^{-1})
K	association equilibrium constant [$=k_{as}/k_{dis}$] (cm^3 mol^{-1})
l	thickness of the polymer layer (cm)
T	temperature (K)
x	distance from the electrode (cm)
Δx	electron hopping distance (cm)
y	dimensionless distance from the electrode [$=x/l$]
Z	partition function
β	$1/k_BT$
δ	average counterion hopping distance (cm)

ϵ	dimensionless interaction energy constant [$=J/k_BT$]
κ	ion pairing constant [$=KC^0$]
λ	dimensionless potential (as in eq10)
ρ	ratio of oxidized to reduced species concentration at t = 0
ρ_M	redox species concentration corresponding to ψ_{LM}
σ	ion pairing constant [$=KC_E^0$]
Φ	potential at a particular site (V)
ϕ	dimensionless potential [$=(e/k_BT)\ \Phi$]
χ_A, χ_B, χ_D	
χ_D and χ_F	fractional concentration of species A, B, C, D, and F respectively
χ_E	molar fraction of electroactive species [as expressed in eq 29
χ_T	total fraction of electron transfer active species [$=\chi_A+\chi_B$]
ψ	dimensionless current [$=I/I_d$]
ψ_{LM}	maximum limiting current

Superscripts

e	equilibrium value
c	corresponding to counterion
ap	apparent value
0	true value

References and Notes

(1) Eisenberg, A. *Macromolecules* **1970**, *3*, 147.
(2) Eisenberg, A.; King, M. In *Ion-Containing Polymers*; Academic Press: New York, 1977.
(3) Komoroski, R. A.; Mauritz, K. A. In *Perfluorinated Ionomer Membranes*; Eisenberg, A., Yeager, H. L., Eds.; American Chemical Society: Washington, DC, 1982; ACS Symposium Series 180; p 118.
(4) Savéant, J.-M. *J. Phys. Chem.* **1988**, *92*, 1011.
(5) Savéant, J.-M. *J. Phys. Chem.* **1988**, *92*, 4526.
(6) Anson, F. C.; Blauck, D. N.; Savéant, J.-M.; Shu, C.-F. *J. Am. Chem. Soc.* **1991**, *113*, 1922.
(7) Nahir, M.; Buck, R. P. *J. Phys. Chem.* **1993**, *97*, 12363.
(8) Denny, R. A.; Sangaranarayanan, M. V. *J. Phys.Chem. B* **1998**, *102*, 2131 and 2138.
(9) Pineri, M., Eisenberg, A., Eds. *Structure and Properties of Ionomers*; D. Reidel Publishing Co.: Dordrecht, The Netherlands, 1987.
(10) (a) Laviron, E.; Roullier, L. *J. Electroanal. Chem.* **1980**, *115*, 65. (b) Laviron, E. *J. Electroanal. Chem.* **1981**, *122*, 37.
(11) Denny, R. A.; Sangaranarayanan, M. V. *Chem. Phys. Lett.* **1995**, *239*, 131.
(12) Denny, R. A.; Sangaranarayanan, M. V. *J. Solid State Electrochem.* **1997**, *2*, 67.
(13) Denny, R. A.; Sangaranarayanan, M. V. *J. Phys. A: Math. Gen.* **1998**, *31*, 7671.
(14) Buck, R. P. *J. Electroanal. Chem.* **1987**, *219*, 23.
(15) Bard, A. J.; Faulkner, L. R. In *Electrochemical Methods: Fundamental and Applications*; John-Wiley: New York, 1980.
(16) Facci, J. S.; Schmehl, R. H.; Murray, R. W. *J. Am. Chem. Soc.* **1982**, *104*, 4960.
(17) Buttry, D. A.; Anson, F. C. *J. Electroanal. Chem.* **1981**, *130*, 333.
(18) He, P.; Chien, X. *J. Electroanal. Chem.* **1988**, *256*, 353.
(19) Fritsch-Faules, I.; Faulkner, L. R. *J. Electroanal. Chem.* **1989**, *263*, 237.
(20) Oyama, N.; Tasuma, T.; Takahashi, K. *J. Phys. Chem.* **1993**, *97*, 10504.
(21) Sharp, M.; Lindholmsethson, R.; Lind, E. L. *J. Electroanal. Chem.* **1993**, *345*, 223.
(22) Sosnoff, C. S.; Sullivan, M.; Murray, R. W. *J. Phys. Chem.* **1994**, *98*, 13643.
(23) Chidsey, C. E. D.; Murray, R. W. *J. Phys. Chem.* **1986**, *90*, 1479.
(24) Laviron, E. *J. Electroanal. Chem.* **1980**, *112*, 1.
(25) Mathias, M. f.; Haas, O. *J. Phys. Chem.* **1992**, *96*, 3174.
(26) Ikeda, T.; Leidner, C. R.; Murray, R. W. *J. Electroanal. Chem.* **1982**, *138*, 343.
(27) Andrieux, C. P.; Haas, O.; Savéant, J.-M. *J. Am. Chem. Soc.* **1986**, *108*, 8175.
(28) Gunton, J. D.; Miguel, M. S.; Sahni, P. S. In *Phase Transition and Critical Phenomena*; Domb, C., Lebowitz, H., Eds.; Academic: London, 1983; Vol. 8.
(29) Glotzer, S. C.; Stauffer, D.; Jan, N. *Phys. Rev. Lett.* **1994**, *72*, 4109.
(30) Bernardesm, A.T.; Liverpool, T. B.; Stauffer, D. *Phys. Rev. E* **1996**, *54*, R2220.
(31) See for example, Velasco, E.; Toxvaerd, S. *Phys. Rev. E* **1996**, *54*, 605.